Proceedings of the 21st ICSMGE, Vienna, Austria, 14 – 19 June 2026. Pistrol, Adam & Schweiger (eds.)
Published by: ÖGG, Austrian Society for Geomechanics, Salzburg, Austria, ISBN 978-3-9503898-4-5
https://doi.org/10.53243/ICSMGE2026-420

Seismic Fragility Analysis of Piled Raft Foundations Under Bi-Directional Motions

Atul Raj, Sumanta Haldar and Shantanu Patra
Department of Civil Engineering, School of Infrastructure, Indian Institute of Technology Bhubaneswar, Khordha, Odisha, India, a22ce09003@iitbbs.ac.in

ABSTRACT: Piled raft foundations (PRFs) are effective engineering solutions used in construction projects to support high-rise buildings and other large structures in earthquake-prone areas, as they combine the benefits of piles and rafts to improve stability and load-bearing capacity. PRFs play a crucial role in mitigating overall and differential settlement, thereby improving the structural stability of buildings. However, their seismic performance remains an area of growing interest, particularly due to the complex interactions between soil, structure, and foundation during earthquake loading. Seismic fragility assessments are essential for evaluating their performance under earthquake loading, providing a probabilistic framework to quantify the likelihood of a system reaching or exceeding predefined damage states. While considerable research has been conducted on the seismic reliability of foundation systems, studies focusing on the fragility of PRF and superstructure system are limited. This study investigates the seismic fragility of PRFs, evaluating their performance and assessing the probability of earthquake-induced damage under bi-directional ground motions. The assessment integrates probabilistic approaches with numerical modelling to assess the likelihood of damage and failure. A three-dimensional (3D) finite element analysis (FEA) is performed in SAP2000. The soil is modelled using API-based nonlinear *p-y*, *t-z*, and *Q-z* springs, with hysteretic behaviour using Takeda model. Piles are modelled as frame elements, while the raft is represented using shell elements. The superstructure is idealised as reinforced concrete frames, and PRF is considered to be embedded in sand. The beams and columns of the superstructure are modelled as frame elements, whereas the slab is modelled using shell elements. Incremental dynamic analyses (IDA) were conducted to develop the seismic fragility curves for distinct damage states for both the superstructure and the PRF under near-field and far-field earthquake motions. The outcome of this study provides a comprehensive evaluation of resilience of piled raft-supported structures against earthquakes.

KEYWORDS: Bi-directional motion; Finite element method; Piled raft foundations; Seismic Fragility; Soil-structure interaction.

1 INTRODUCTION

Piled raft foundations (PRFs) are often used to support high-rise buildings, bridges, towers, and nuclear power plants because they effectively share the load among the raft and piles. Including piles beneath raft plays an important role in reducing settlement, which helps improve structural stability while also lowering the overall foundation cost (Poulos 2001). Compared to conventional pile group and raft foundation, PRF offer significant advantages, as it allows for strategic control of the length, diameter and location of pile, which leads to improved foundation design. This optimisation helps in reducing both differential and total settlements while enhancing the bearing capacity without incurring excessive costs (Mandolini et al. 2005 and de Sanctis & Russo 2008). Their application has grown over the past 20 years as a result of the unavailability of land and the need for economical and safe foundations on various soils, particularly in seismically active regions (Raj et al. 2024). Burland & de Mello (1977) initially proposed an effective design method of placing piles beneath the raft foundation to control settlements beyond acceptable limits. Subsequently, more studies have examined PRF behaviour, resulting in various design recommendations and guidelines (Randolph 1994 and Horikoshi & Randolph 1998). Many countries have adopted combined PRFs because they perform well under both static and seismic loading (Katzenbach et al. 2000, Katzenbach et al. 2016, Reul & Randolph 2004, and Bhaduri & Choudhury 2020). However, due to the complex interactions among piles, raft, superstructure and soil, the design of PRF for seismic loads is quite challenging (Varghese et al. 2020). In seismically active areas, the behaviour of PRFs is even more complicated due to the dynamic nature of seismic loading.

Traditionally, seismic design of PRF-based structures usually assumes a fixed base condition and ignores the effects of soil-structure interaction (SSI). The main reason for this approach is the complexity of modelling complete soil-foundation-structure system and lack of standardised and validated analysis techniques (Chaudhuri et al. 2020). The simplified assumption of ignoring SSI is considered acceptable for specific types of structures and soil conditions, particularly lightweight structures founded on stiff soils (Alavi & Alidoost 2012). However, the influence of SSI is significant for heavy structures supported on soft or loose soils. In such scenarios, ignoring SSI effects may result in unsafe designs for both the superstructure and the foundation, as demonstrated by several past earthquake case studies (Bagheri et al. 2018, Chanda et al. 2025). Several major seismic codes, including ATC (1978), ASCE 7-16 (2017), Eurocode 8 Part 1 (2005), Eurocode 8 Part 5 (2004), JSCE (2015), and NZS 1170-5 (2005), incorporate provisions for SSI in a range of structural systems such as abutments, caissons, pile-supported foundations, and retaining walls, yet explicit and comprehensive guidance for addressing SSI in the seismic design of combined PRF remain insufficient and require further investigation. The recent IS 19117 (2025) outlines recommended limits for pile geometry, spacing, and stiffness ratios in combined PRF, helping ensure realistic load-sharing and settlement performance. It also emphasises the importance of considering SSI and both inertial and kinematic effects when evaluating combined PRFs under seismic loading. Most studies on the seismic performance of PRFs in sandy and clayey soils have primarily relied on shake table tests, centrifuge experiments, and numerical simulations, with a strong emphasis on sinusoidal ground motions of varying frequencies and amplitudes (Matsumoto et al. 2004, Yuksekol et al. 2015 and Bhaduri & Choudhury 2021). On the other hand, some researchers have examined PRFs under earthquake conditions, employing both recorded and artificial ground motions (Bhaduri et al. 2020, and Saha et al. 2020). Numerous case studies have investigated the efficacy of PRFs in sustaining superstructures during significant earthquakes (Onimaru et al. 2012, and Yamashita et al. 2012). Furthermore, various past studies (Badry & Satyam 2017 and Firoj & Maheshwari 2022) have investigated the dynamic response of PRF with respect to the overlying superstructure. Although the response of PRFs under seismic loading has been extensively studied, most of these studies focus on unidirectional ground motions, which cannot adequately capture the complexity of actual earthquake

loading. While these studies provide valuable information, the effect of bidirectional seismic loading on PRF remains underexplored despite its practical importance in seismic design.

Most of the existing research approximates the superstructure as a lumped mass or as a single degree of freedom system. Although this approach simplifies the analytical process, it does not adequately capture the full complexity of the dynamic interaction that exists between structure and foundation system. These simplifications tend to exclude the most important factors, such as mass distribution, stiffness irregularities, and complex interactions among structural elements, which may lead to inaccurate predictions of the overall seismic response. Hence, to more accurately evaluate the seismic response of PRF, a more realistic description of the superstructure is essential. A comprehensive understanding of seismic response is crucial as it directly affects casualties and economic losses resulting from earthquake events. Correct prediction of earthquake-induced damage and building performance is a crucial part of effective seismic risk analysis (Kohns et al. 2022). In this regard, vulnerability assessment, the relationship between seismic intensity and the likelihood of structural damage or failure, is an important factor. The vulnerability is typically quantified through seismic fragility analysis within the framework of performance-based earthquake engineering. The method was first introduced by Kennedy et al. (1980) during a probabilistic seismic assessment of a nuclear power plant. Seismic fragility refers to the probability that a structural component or system will exceed a predefined damage state (DS) when subjected to a certain intensity of earthquake (Porter et al. 2007).

Despite growing research on the seismic performance of PRFs, several important aspects remain underexplored. Most of the previous studies have overlooked essential aspects like SSI, effects of bi-directional seismic loading, and influence of realistic superstructure modelling. Use of simplified models such as fixed-base assumptions, unidirectional ground motions, or lumped-mass superstructures limits the ability to accurately predict the dynamic behaviour and potential damage of PRF-supported structures during earthquakes.

To address these limitations, this study examines the seismic fragility of PRFs, evaluating their performance under bidirectional earthquake ground motions. Three-dimensional finite element analysis was conducted using SAP2000, where soil is represented by API-based nonlinear *p-y*, *t-z*, and *Q-z* springs, incorporating hysteretic behaviour through the Takeda model. The superstructure was idealised as reinforced concrete frames, and PRF was considered to be embedded in sand. The beams, piles, and columns were represented as frame elements, whereas the raft and slab were modelled using shell elements. A series of incremental dynamic analyses was performed using both far-field and near-field earthquakes to evaluate the seismic response. The study then develops fragility curves for different damage states for both superstructure and PRF. The outcome provides probabilistic understanding of damage likelihood and structural resilience, contributing to improved seismic risk assessment and design strategies for PRF-supported buildings.

2 FINITE ELEMENT MODELLING

A three-dimensional (3D) finite element (FE) analysis of 10-storey reinforced concrete (RC) building supported on PRF is performed using FE software, SAP2000v20 (SAP 2000). The building has a fundamental period of 1.0 second under fixed-base conditions (T_{fixed}), which is representative of a 10-storey building, as per ASCE 7-16 (2017). The schematic diagram and plan view of PRF are shown in Figure 1. The building had square floor plan (12 m × 12 m) and three bays in both the X and Y directions with a 3 m storey height. As shown in Figure 2, each floor is modelled as a rigid slab, supported horizontally by eight beams and vertically by sixteen columns. Frame elements were used to model the beams and columns, while shell elements were utilised for the slab. The natural period of the building under fixed-base conditions (T_{fixed}) is obtained using modal analysis by adjusting the structural member's stiffness. The PRF comprises 16 piles (diameter = 1.5 m and length = 15 m) arranged in a 4 × 4 configuration and constructed using M40 grade concrete. These piles are modelled as nonlinear frame elements, with assigned P-M2-M3 hinges to capture their flexural and axial nonlinear behaviour under seismic loading. The rectangular raft (18 m × 16 m × 2.5 m) is modelled using shell elements. The PRF configuration used in this study lies within the limits specified in IS 19117 (2025), including pile slenderness, spacing, and stiffness characteristics.

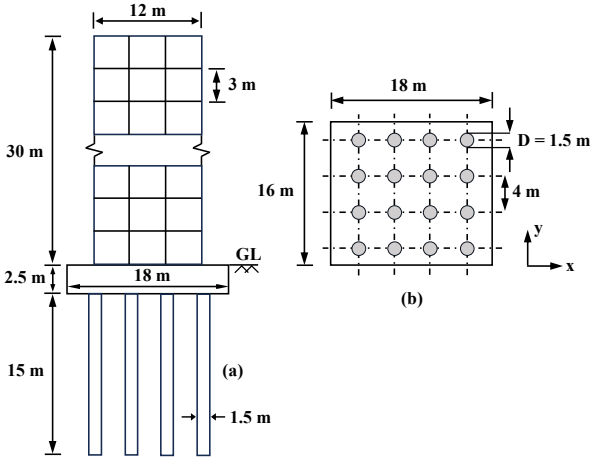

Figure 1. (a) Schematic representation of 10-storey building supported on PRF, (b) Plan view of PRF.

Following the method suggested by Saha et al. (2015), distributed springs were attached at each raft's node in three translational directions to simulate the raft-soil interaction. According to Dutta et al. (2008), this distributed spring approach provides a more realistic representation of SSI compared to earlier methods, such as those proposed by Gazetas (1991), where equivalent springs were placed at the centroid of the foundation for each degree of freedom. The values of spring stiffness in lateral, longitudinal, and vertical directions were determined based on established formulations and guidelines available in the literature (Dutta et al. 2008), ensuring appropriate simulation of the raft-soil interaction. Nodes on the raft were generated by discretising the raft into square grids of 0.5 m mesh size. The chosen mesh size was found through a sensitivity analysis to provide convergence and accuracy in the responses. The pile-soil interaction was represented utilising *p-y*, *t-z*, and *Q-z* springs, in accordance with the American Petroleum Institute (API) guidelines (API 2011). In order to simulate lateral resistance, the *p-y* springs were assigned in two orthogonal directions, whereas shaft friction and tip resistance were simulated through *t-z* and *Q-z* springs, respectively. The *p-y* and *t-z* springs were uniformly distributed along the pile's length at 1 m intervals. These springs are modelled using Multi-Linear Plastic (MLP) link elements, with hysteretic behaviour defined by the Takeda model. A damping ratio of 5% was considered. Properties for soil and concrete were obtained from established literature (Neville 2011, Raj et al. 2025), as detailed in Table 1.

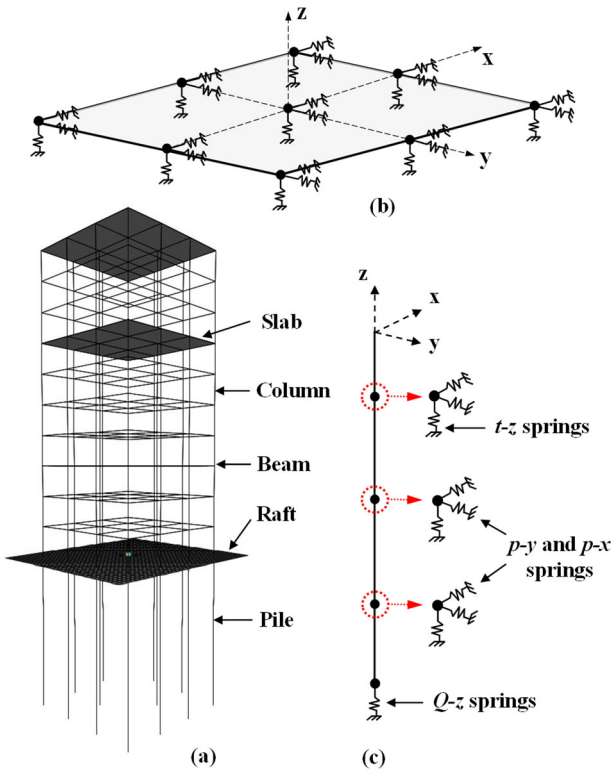

Figure 2. (a) FE model, (b) Soil-raft modelling, (c) Soil-pile modelling.

Table 1. Soil and concrete properties used in the present study.

Parameters	Symbol/Unit	Ottawa Sand	Concrete
Effective unit weight	γ' (kN/m^3)	15.3	25
Young's modulus	E (MPa)	20	31622
Poisson's ratio	μ	0.3	0.2
Friction angle	ϕ (°)	32	-
Relative density	%	45	-

2.1 *Validation of Numerical Model*

The accuracy and reliability of numerical model were verified using experimental results presented by Chau et al. (2009). A shake table test was performed by Chau et al. (2009) on a single-storey steel structure. The test setup was modelled in SAP2000, with soil-structure interaction captured using MultiLinear Plastic (MLP) links. The 1940 El Centro earthquake, which had a PGA of 0.135g, was employed for Nonlinear Time History Analysis (NTHA). Figure 3 presents a comparison between the top floor acceleration obtained from the simulation and experimental measurements, demonstrating a strong correlation. This confirms accuracy and effectiveness of numerical model in capturing SSI behaviour.

3 SELECTION OF GROUND MOTIONS

Ten earthquake records were selected to evaluate the seismic vulnerability of the PRF system, comprising five near-field (NF) and five far-field (FF) earthquakes. Earthquake records were obtained from the Pacific Earthquake Engineering Research (PEER) database (https://ngawest2.berkeley.edu). Each record comprises of two horizontal components: longitudinal (H_1) and transverse (H_2). The properties of the earthquakes are presented in Tables 2 and 3 for the near-field and far-field earthquakes, respectively. Near-field earthquakes are typically observed within 20 km of the fault rupture and are often associated with high-velocity pulses that markedly amplify their destructive effects (Yadav & Gupta 2017). These velocity pulses result from fault rupture dynamics and directivity effects. These pulse-like motions are known to significantly influence structural responses.

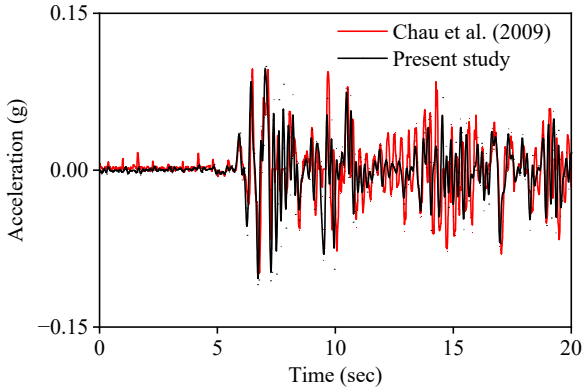

Figure 3. Comparison of acceleration response between FE model and results from Chau et al. (2009).

Table 2. Properties of selected near-field earthquakes.

Earthquake Name	Year	Station Name	M	R_{jb} (km)	PGA (H_1) (g)	PGA (H_2) (g)	T_{Pulse} (sec)
Imperial Valley-06	1979	El Centro Array #6	6.53	0	0.449	0.447	3.77
Irpinia	1980	Sturno (STN)	6.9	6.78	0.320	0.227	3.27
Kobe	1995	Port Island (0 m)	6.9	3.31	0.348	0.289	2.83
Kocaeli	1999	Yarimca	7.51	1.38	0.322	0.227	4.95
Denali	2002	TAPS Pump Station #10	7.9	0.18	0.333	0.297	3.16

Table 3. Properties of selected far-field earthquakes.

Earthquake Name	Year	Station Name	M	R_{jb} (km)	PGA (H_1) (g)	PGA (H_2) (g)
Superstition Hills-02	1987	Imperial Valley Wildlife Liquefaction Array	6.54	23.85	0.208	0.179
Manjil	1990	Abhar	7.37	75.58	0.209	0.132
Hector Mine	1999	San Bernardino - E & Hospitality	7.13	105.2	0.073	0.058
Chi-Chi	1999	CHY094	6.2	47.55	0.028	0.022
Iwate	2008	AKTH16	6.9	61.19	0.111	0.107

4 METHODOLOGY

This study uses numerical modelling and probabilistic assessment techniques to evaluate the seismic vulnerability of a 10-storey RC building supported on PRF. The approach involves two significant steps: (i) performing Incremental Dynamic Analysis (IDA), and (ii) developing fragility curves. A set of 10 real earthquake records from both NF and FF was utilised to represent different earthquake characteristics. Using SAP2000, 3D FE models were created to capture their dynamic behaviour under seismic loading. The models include detailed representations of the superstructure, PRF and soil-structure interactions. After establishing the models, IDA analyses were conducted to evaluate the nonlinear response at higher earthquake intensities. IDA was initially proposed by Bertero (1977) and subsequently elaborated by Vamvatsikos & Cornell (2002), involves conducting a series of NTHA with multiple

earthquake records, each scaled incrementally to represent different seismic intensity levels. The selection of IM is important in seismic fragility analysis because it greatly influences the scaling process in IDA as well as the expression of ground motion severity. PGA is widely used because of its effectiveness and convenience; thus, it is used in the current study. The PGA values employed in the current study range between 0.2g and 1.2g with an increment of 0.2g. The selected IMs were used to develop seismic fragility curves, which express the probability of exceedance (POE) of certain thresholds at different levels of ground motion. Fragility is commonly represented using a lognormal probability distribution and expressed by Equation 1 as:

$$P(\, ds \geq ds_i \mid IM\,) = \Phi\left[\frac{1}{\beta_t} ln\left(\frac{IM}{IM_m}\right)\right] \quad (1)$$

where, $P(ds \geq ds_i|IM)$ = the probability of exceedance of specific damage state (DS) ds_i, for a given IM. Φ = standard cumulative probability function, IM_m = median value of IM corresponding to the i^{th} DS threshold, β_t = standard deviation of fragility function. For generating fragility curves of different DS, this study developed a probabilistic seismic demand model (PSDM) using regression analysis. Engineering demand parameters (EDPs) were extracted from IDA to represent the structural response under varying seismic intensities. The resulting PSDM was then combined with the defined capacity thresholds to calculate the probability of exceedance (POE) for each DS based on the specified limit value for the corresponding damage measures (DMs).

In the present study, focus is on evaluating seismic fragility of system when subjected to bidirectional ground motions. To achieve this, damage measures (DMs) are established based on engineering demand parameters (EDPs) that are pertinent to both the superstructure and the foundation components. The selected DM include Maximum Inter-storey Drift Ratio (MIDR), representing response of superstructure, and two parameters related to the PRF system: maximum bending moment in the piles (BM_{max}) and maximum raft displacement ($\delta_{raft,max}$). For each DM, three damage states, slight, moderate, and severe, were taken into consideration. The permissible values for MIDR were taken from FEMA 356 (2000), while the limits for BM_{max} and $\delta_{raft,max}$ were derived from pushover analysis as per Kohns et al. (2022) and are given in Table 4.

Table 4. Damage states for various damage measures used in the present study.

Damage Measures	Damage States		
	Slight	Moderate	Severe
Maximum Inter-storey Drift Ratio	1%	2%	4%
Maximum bending moment in piles	$0.25BM_{max}$	$0.57BM_{max}$	BM_{max}
Maximum raft displacement	$0.1\delta_{raft,max}$	$0.25\delta_{raft,max}$	$\delta_{raft,max}$

5 RESULTS AND DISCUSSION

Seismic fragility of 10-storey RC building supported on a PRF is assessed through detailed NTHA, focusing on three key EDPs: MIDR, BM_{max}, and $\delta_{raft,max}$. These damage measures represent critical performance indicators at both the superstructure and foundation levels. For each of these EDPs, IDA curves and fragility curves are developed under both near-field and far-field earthquakes.

5.1 *Incremental Dynamic Analysis*

IDA was conducted using a suite of recorded NF and FF earthquake motions applied in both horizontal directions. IDA curves are generated for each damage measure to understand the behaviour of the structure as seismic intensity increases. Figures 4a, 4b and 4c show IDA curves illustrating the variation of MIDR, BM_{max}, and $\delta_{raft,max}$, respectively, for both NF and FF earthquakes. The responses to NF and FF earthquakes show differences across all three damage measures. The mean values of responses are consistently higher when subjected to NF ground motions, indicating a greater seismic demand. The factor contributing to these increased responses is the presence of strong velocity pulses with longer periods in NF events. These pulses, characterised by higher energy content, are capable of delivering substantial lateral forces to a structure. As a result, for the same PGA, NF earthquakes tend to induce more significant responses than FF earthquakes. This underscores the necessity of considering near-field effects in seismic design and evaluation, especially for structures situated near active fault zones.

5.2 *Fragility Analysis*

Seismic fragility curves were constructed by plotting the probability of exceedance (POE) for various DS against PGA. Figures 5a, 5b and 5c illustrate the seismic fragility curves for different DS corresponding to three selected damage measures, MIDR, BM_{max}, and $\delta_{raft,max}$, respectively, under NF and FF earthquakes. The fragility curves show a consistent trend of higher POE under NF ground motions compared to FF across all damage states. The difference in the POE between NF and FF earthquakes tends to increase progressively from slight to severe damage state across all evaluated damage measures. This trend highlights the influence of earthquake type becomes more significant as the level of structural damage intensifies. In order to explore this further, the POE is analysed at three different PGA levels, 0.2g (low), 0.5g (medium), and 0.8g (high), to compare responses under NF and FF earthquake motions. At lower earthquake intensities, the difference in POE for slight and severe is 23.7% for NF and 11.7% for FF for the considered damage measure, MIDR. The difference becomes 21% and 6.8% for maximum BM and 4.5% and 0.7% for maximum raft displacement for NF and FF earthquakes, respectively. For medium earthquakes, the variation between POE for slight and severe becomes 59.8% and 47.1% for NF and FF earthquakes for MIDR. The difference becomes 68.1% and 46.4% for maximum BM and 33.1% and 15% for maximum raft displacement. For high-intensity earthquakes, the difference is in the order of 68.2% and 75.9% for MIDR, 77.8% and 84.2% for maximum BM and 78.8% and 63.9% for maximum raft displacement when subjected to NF and FF earthquakes. The outcomes of the analysis show that both maximum BM in piles and MIDR are sensitive and comparable in identifying slight damage. However, as the damage level increases, MIDR becomes more sensitive. This trend remains consistent for both NF and FF earthquakes.

6 CONCLUSIONS

This study develops seismic fragility curves for a 10-storey RC building supported on a PRF. The analysis considered both NF and FF earthquakes to evaluate structural and foundation performance under varying seismic intensities. 3D numerical modelling was done in FE software SAP2000. Incremental dynamic analysis was carried out to develop the fragility curves for both the superstructure and the piled raft foundation. Based on the results, the following conclusions can be drawn:

- The mean values of responses are consistently higher when subjected to NF earthquakes, indicating a greater seismic demand.
- The fragility curves show a consistent trend of higher POE under NF ground motions compared to FF across all damage states. This is due to the presence of strong velocity pulses with longer periods in near-field events.
- The result shows that both the maximum bending moment in piles and MIDR are sensitive and comparable in identifying slight damage. However, as the damage level increases, MIDR becomes more sensitive. This trend is consistent for both NF and FF earthquakes.

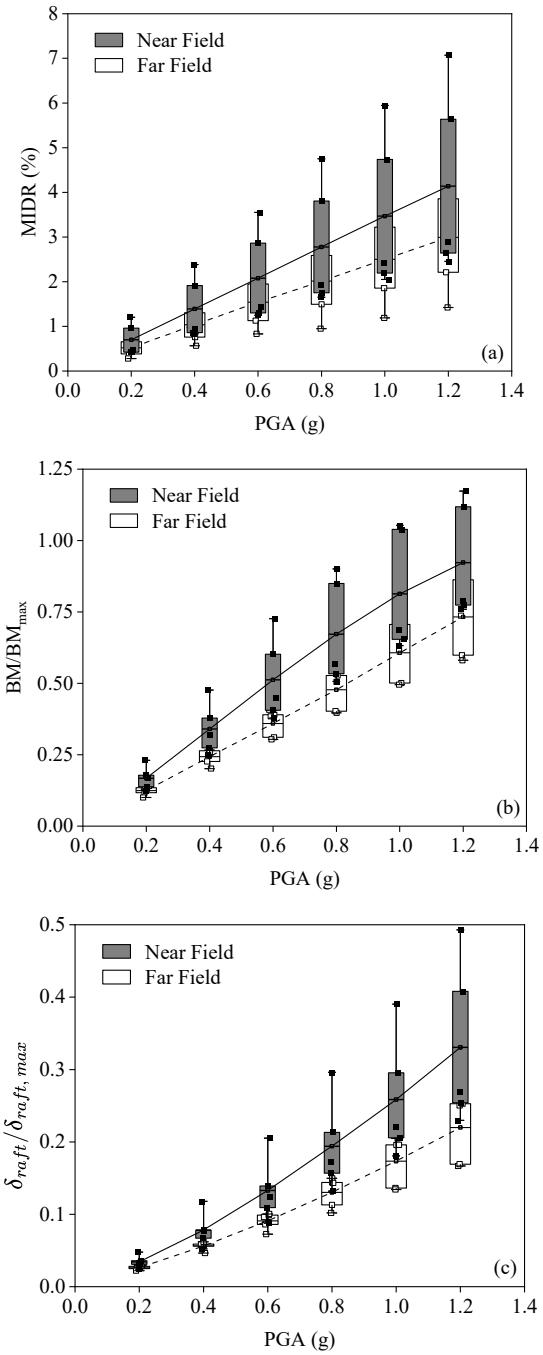

Figure 4. Distribution of (a) MIDR, (b) Maximum bending moment in piles, (c) Maximum raft displacement, across PGA levels under NF and FF earthquakes.

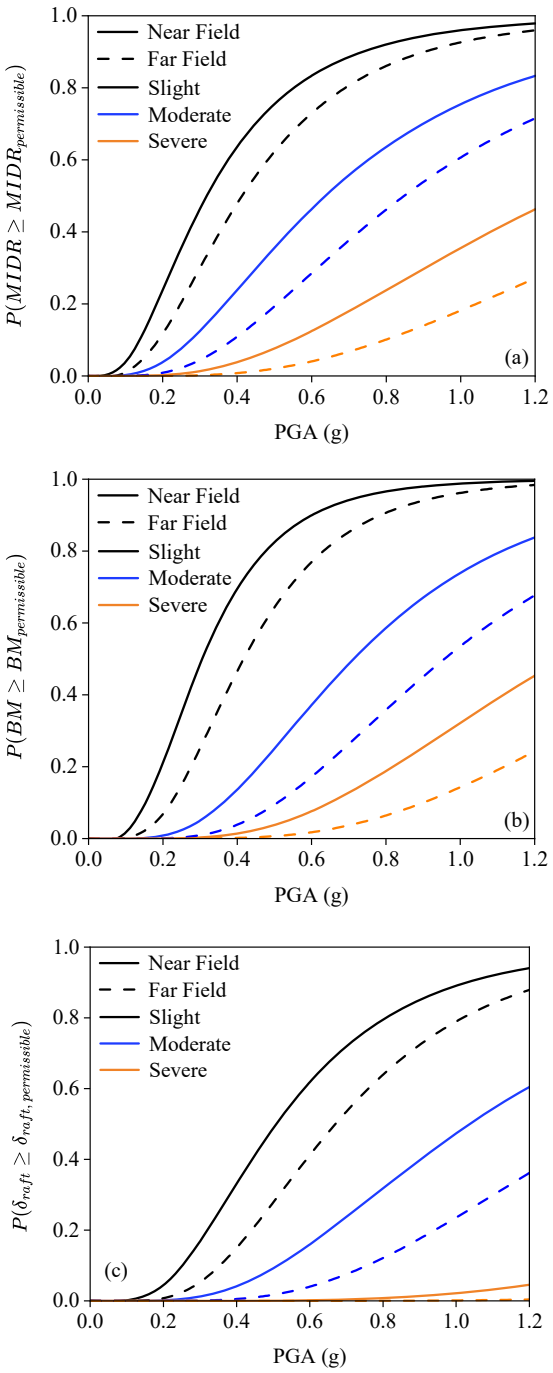

Figure 5. Seismic fragility curves for (a) MIDR, (b) Maximum BM in piles, (c) Maximum raft displacement, under near-field and far-field earthquakes across three damage states.

Based on the observed results, it is recommended that seismic design practices and fragility evaluations for structures supported on piled raft foundations account for both the type of earthquake (NF and FF) and bidirectional ground motion. These factors have a notable impact on responses and can significantly affect the likelihood of exceeding damage thresholds.

Although the fragility analysis in this study was based on ten earthquake records, the findings offer meaningful insights. For a more comprehensive understanding of seismic performance, future studies should incorporate a higher number of ground motions. Additionally, investigating the effects of different soil properties, pile configurations, and structural irregularities would further enhance insights into the behaviour of PRF during earthquake loading.

7 REFERENCES

Alavi, E. and Alidoost, M., 2012, September. Soil-structure interaction effects on seismic behavior of base-isolated buildings. In *Proc. of 15th World Conference on Earthquake Engineering, Portugal*.

API-RP-2GEO. 2011. Geotechnical and foundation design considerations. *American Petroleum Institute RP 2GEO*, Washington, DC, USA.

Applied Technology Council and Structural Engineers Association of California, 1978. *Tentative provisions for the development of seismic regulations for buildings: A cooperative effort with the design professions, building code interests, and the research community* (Vol. 3, No. 6). US Department of Commerce, National Bureau of Standards.

ASCE 7_16 2017. Minimum Design Loads and Associated Criteria for Buildings and Other Structures. *American Society of Civil Engineers*.

Badry, P. and Satyam, N., 2017. Seismic soil structure interaction analysis for asymmetrical buildings supported on piled raft for the 2015 Nepal earthquake. *Journal of Asian Earth Sciences*, *133*, pp.102-113.

Bagheri, M., Jamkhaneh, M.E. and Samali, B., 2018. Effect of seismic soil–pile–structure interaction on mid-and high-rise steel buildings resting on a group of pile foundations. *International Journal of Geomechanics*, *18*(9), p.04018103.

Bertero, V.V., 1977. Strength and deformation capacities of buildings under extreme environments. *Structural engineering and structural mechanics*, *53*(1), pp.29-79.

Bhaduri, A. and Choudhury, D., 2020. Serviceability-based finite-element approach on analyzing combined pile–raft foundation. *International Journal of Geomechanics*, *20*(2), p.04019178.

Bhaduri, A. and Choudhury, D., 2021. Steady-state response of flexible combined pile-raft foundation under dynamic loading. *Soil Dynamics and Earthquake Engineering*, *145*, p.106664.

Bhaduri, A., Rao, V.D. and Choudhury, D., 2020. The behaviour of pile group and combined piled-raft foundation in liquefiable soil under seismic conditions. *Geotechnical Engineering Journal of the SEAGS & AGSSEA*, *51*(2), pp.130-138.

Burland, J.B., Broms, B.B. and De Mello, V.F., 1978. Behaviour of foundations and structures.

Chanda, D., Saha, R. and Haldar, S., 2025. Seismic behaviour of RC framed building supported on combined piled raft foundation in sandy soil. *Arabian Journal for Science and Engineering*, *50*(3), pp.2057-2089.

Chau, K.T., Shen, C.Y. and Guo, X., 2009. Nonlinear seismic soil–pile–structure interactions: shaking table tests and FEM analyses. *Soil Dynamics and Earthquake Engineering*, *29*(2), pp.300-310.

Chaudhuri, C.H., Chanda, D., Saha, R. and Haldar, S., 2020, December. Three-dimensional numerical analysis on seismic behavior of soil-piled raft-structure system. In *Structures* (Vol. 28, pp. 905-922). Elsevier.

CSI Analysis Reference Manual for SAP. Version 20.0.0, Computers and Structures, IN; 2000.

de Sanctis, L. and Russo, G., 2008. Analysis and performance of piled rafts designed using innovative criteria. *Journal of geotechnical and geoenvironmental engineering*, *134*(8), pp.1118-1128.

Dutta, S.C., Bhattacharya, K. and Roy, R., 2008. Effect of flexibility of foundations on its seismic stress distribution. *Journal of Earthquake Engineering*, *13*(1), pp.22-49.

EN, B., 2004. Eurocode 8: Design of structures for earthquake resistance-*Part 5*: Foundations, retaining structures and geotechnical aspects.

FEMA. 2000. Prestandard and commentary for seismic rehabilitation of buildings. FEMA 356. Washington, DC: FEMA

Firoj, M. and Maheshwari, B.K., 2022. Effect of CPRF on nonlinear seismic response of an NPP structure considering raft-pile-soil-structure-interaction. *Soil Dynamics and Earthquake Engineering*, *158*, p.107295.

Gazetas, G., 1991. Formulas and charts for impedances of surface and embedded foundations. *Journal of geotechnical engineering*, *117*(9), pp.1363-1381.

Horikoshi, K. and Randolph, M.F., 1998. A contribution to optimum design of piled rafts. *Geotechnique*, *48*(3), pp.301-317.

Indian Standard: 19117 (2025) Design and construction of combined piled-raft foundations-code of practice*. Bureau of Indian Standards*, New Delhi.

JSCE 15, 2015. Standard specifications for concrete structures-design, Tokyo: *Japan Society of Civil Engineers*.

Katzenbach, R., Arslan, U. and Moormann, C., 2000. 13. Piled raft foundation projects in Germany. *Design applications of raft foundations*, *323*.

Katzenbach, R., Leppla, S. and Choudhury, D., 2016. *Foundation systems for high-rise structures*. CRC press.

Kennedy, R.P., Cornell, C.A., Campbell, R.D., Kaplan, S. and Perla, H.F., 1980. Probabilistic seismic safety study of an existing nuclear power plant. *Nuclear engineering and design*, *59*(2), pp.315-338.

Kohns, J., Stempniewski, L. and Stark, A., 2022. Fragility functions for reinforced concrete structures based on multiscale approach for earthquake damage criteria. *Buildings*, *12*(8), p.1253.

Mandolini, A., Russo, G. and Viggiani, C., 2005. Pile foundations: Experimental investigations, analysis and design. In *Proceedings of the 16th International Conference on Soil Mechanics and Geotechnical Engineering* (pp. 177-213). IOS Press.

Matsumoto, T., Fukumura, K., Horikoshi, K. and Oki, A., 2004. Shaking table tests on model piled rafts in sand considering influence of superstructures. *International Journal of Physical Modelling in Geotechnics*, *4*(3), pp.21-38.

Neville, A. M. 2011. *Properties of concrete*. Pearson Education India.

NZS 1170-5, 2004. Structural design actions-part 5: earthquake actions - New Zealand, *Wellington: Standards New Zealand*.

Onimaru, S., Hamada, J., Nakamura, N. and Yamashita, K., 2012. Dynamic soil-structure interaction of a building supported by piled raft and ground improvement during the 2011 Tohoku Earthquake. In *Proc. 15 the World Conference of Earthquake Engineering*.

PEER Ground Motion Database n.d. https://ngawest2.berkeley.edu.

Porter, K., Kennedy, R. and Bachman, R., 2007. Creating fragility functions for performance-based earthquake engineering. *Earthquake spectra*, *23*(2), pp.471-489.

Poulos, H.G., 2001. Piled raft foundations: design and applications. *Geotechnique*, *51*(2), pp.95-113.

Raj, A., Haldar, S. and Patra, S., 2024, December. Seismic Demand of Piled Raft Foundations Under Bidirectional Earthquake. In *International Conference on Recent Advances in Geotechnical Earthquake Engineering and Soil Dynamics* (pp. 73-83). Singapore: Springer Nature Singapore.

Raj, A., Haldar, S. and Patra, S., 2025, April. Subgrade modulus distribution and load-sharing in piled raft foundations under VHM loading. In *Structures* (Vol. 74, p. 108569). Elsevier.

Randolph, M.F., 1994. Design methods for pile group and piled rafts. In *Proc. 13th Int. Conf. on SFE, 1994* (Vol. 5, pp. 61-82).

Reul, O. and Randolph, M.F., 2004. Design strategies for piled rafts subjected to nonuniform vertical loading. *Journal of Geotechnical and Geoenvironmental Engineering*, *130*(1), pp.1-13.

Saha, R., Dutta, S.C. and Haldar, S., 2015. Effect of raft and pile stiffness on seismic response of soil-piled raft-structure system. *Struct. Eng. Mech*, *55*(1), pp.161-189.

Saha, R., Dutta, S.C., Haldar, S. and Kumar, S., 2020, August. Effect of soil-pile raft-structure interaction on elastic and inelastic seismic behaviour. In *Structures* (Vol. 26, pp. 378-395). Elsevier.

Standard, B., 2005. Eurocode 8: Design of structures for earthquake resistance. *Part*, *1*, pp.1998-1.

Vamvatsikos, D. and Cornell, C.A., 2002. Incremental dynamic analysis. *Earthquake engineering & structural dynamics*, *31*(3), pp.491-514.

Varghese, R., Boominathan, A. and Banerjee, S., 2020. Stiffness and load sharing characteristics of piled raft foundations subjected to dynamic loads. *Soil Dynamics and Earthquake Engineering*, *133*, p.106117.

Yadav, K.K. and Gupta, V.K., 2017. Near-fault fling-step ground motions: Characteristics and simulation. *Soil Dynamics and Earthquake Engineering*, *101*, pp.90-104.

Yamashita, K., Hamada, J., Onimaru, S. and Higashino, M., 2012. Seismic behavior of piled raft with ground improvement supporting a base-isolated building on soft ground in Tokyo. *Soils and Foundations*, *52*(5), pp.1000-1015.

Yuksekol, Y.U., Matsumoto, T. and Shimono, S., 2015, November. Shaking table tests of piled raft and pile group foundations in dry sand. In *Proceedings of 6th International conference on earthquake geotechnical engineering* (Vol. 1).